Organic & Biomolecular Chemistry

Accepted Manuscript

ROYAL SOCIETY OF CHEMISTRY

www.rsc.org/obc

Journal Name

RSCPublishing

ARTICLE

Tailoring Fluorescent Strigolactones for *in vivo* Investigations: a computational and experimental study

Cite this: DOI: 10.1039/xoxxooooox

Received ooth January 2012,
Accepted ooth January 2012

DOI: 10.1039/xoxxooooox

www.rsc.org/

Cristina Prandi,[a] Giovanni Ghigo,[a] Ernesto G. Occhiato,[b] Dina Scarpi,[b] Stefano Begliomini,[b] Beatrice Lace,[a,c] Gabriele Alberto,[a] Emma Artuso,[a] Marco Blangetti[a]

Strigolactones (SLs) are a new class of plant hormones whose role has been recently defined in shoot branching, root development and architecture, and nodulation. They are also active in the rhizosphere as signalling molecules in the communication between plants, AMF (arbuscular mycorrhizal fungi) and parasitic weeds. In spite of the crucial and multifaceted biological role of SLs, the current knowledge on the SL biosynthetic pathway and perception/transduction mechanism is still incomplete. Both genetic and molecular approaches are required to understand the molecular mechanism by which SLs regulate plant development. Our contribution to this topic is the design and synthesis of fluorescent labelled SLs analogues to be used as probes for the detection *in vivo* of the receptor(s). Knowledge of the putative receptor structure will boost the research on analogues of the natural substrates as required for agricultural applications.

Introduction

Since 2008, when their role in controlling shoot branching has been discovered,[1, 2]Strigolactones (SLs) have been identified as a new class of plant hormones playing a pivotal role in plants as modulators of a coordinated development in response to nutrient deficiency conditions.[3, 4]SLs also act as signalling molecules in the rhizosphere. For more than 40 years they have been known to be involved in plant-parasite interactions;[5] more recently SLs have been shown to be key molecules in the communication with arbuscular mycorrhizal fungi (AMF), as they stimulate the hyphal branching of AMF[6] and in the establishment of the beneficial symbiosis with nitrogen-fixing bacteria.[7] The dual role of SLs as endogenous regulators from one side and exogenous signals in the rhizosphere for microbial symbioses development on the other, highlights how SLs could be considered a fascinating class of molecules crucial to mediate adaptive evolution in plants to respond to environmental changes. Even more recently, an antiproliferative activity on cancer cell lines of SLs and analogues has been demonstrated.[8]

All the natural SLs share as common framework (Figure 1) a tricyclic fuse system (ABC) linked to a methyl butenolide through an enol ether bridge (D). The results so far acquired strongly suggest that the biological activity is induced *via* a receptor-mediated mechanism.[9] The mechanism of SL perception occurring at the receptor site is still under discussion. SAR (structure-activity relationship) studies demonstrated that there are nuances between the plant, fungal and parasitic weed systems with respect to SLs' activity.[10, 11] In addition to natural SLs, a number of synthetic analogues have been described,[12-17] whose structure is generally simpler than natural compounds but still retains the enol ether bridge. Besides analogues, synthetic SLs mimics lack both the enol ether moiety and the ABC ring system, and are compounds formed by a butenolide (D ring in SLs) with a good leaving group at C2'. Biological assays using SLs mimics demonstrated that these simple molecules show activity as hormones in plants and as seed germination stimulants.[5, 18, 19] To date, the differences observed in the response of parasitic weeds, fungi and plants for the hormonal activity, suggest that each system uses distinct perception system. Thus, it seems evident that more structure-activity data are needed to

elucidate the mechanism involved in the perception/signalling of SLs and direct the syntheses towards molecules specifically targeted for each of the various roles of SLs.

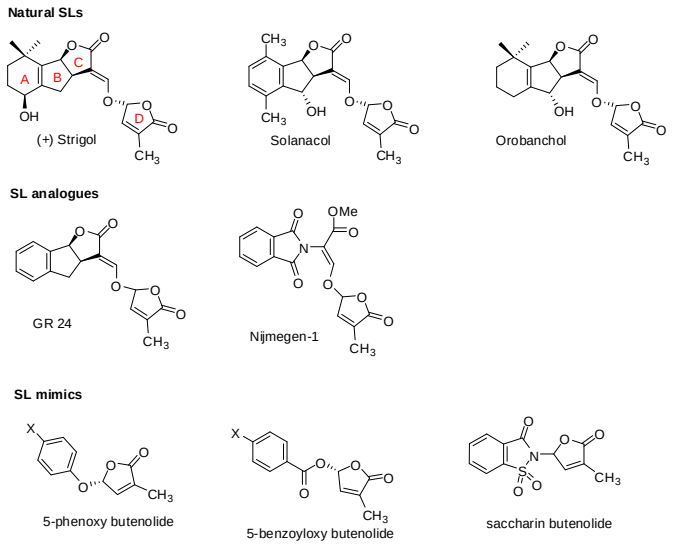

Figure 1

We recently reported on the synthesis of a new class of SLs analogues showing interesting luminescent properties.[12, 20] Our interest in developing new synthetic SLs analogues was focused on two main aims: a) deepen the structure-activity relationship in different systems for each of the different roles ascribed to SLs and b) design fluorescent active SLs analogues suitable for bioimaging studies and *in vivo* detection as a tool to localize the SLs receptor in plant and fungi. Accordingly, in this work we undertook an investigation to predict the spectroscopic properties of new SL analogues and mimics. Among the proposed structures, and on the basis of the calculated fluorescent properties, we then selected some molecules which were consequently synthesized and whose spectroscopic properties measured. Eventually, biological activity tests and preliminary observation *in vivo* were performed confirming that these structures can be considered as a valuable tool for bioimaging applications and, furthermore a good starting point to develop new suitably targeted molecular probes.

Results and Discussion

Computational predictions

In our previous work,[20] we focused our syntheses on nitrogen-containing analogues that showed promising luminescent properties associated with a remarkable bioactivity. In order to better tune the spectroscopic features and to meet the instrumental requirements that fix at 405 nm the minimum wavelength of excitation required for confocal studies, we designed further analogues by modifying/introducing suitable substituents on the aromatic ring, on the ground that modifications at that position have little or no effect on bioactivity. Regrettably, even though the biological activity was satisfactory, the spectroscopic properties were not suitable for applications, as in particular the λ_{max} absorption remained substantially unchanged.[12] At the light of our previous work and considering the need of highlighting the suitable spectroscopic features, we decided to undertake a preliminary screening by computational methods. Purpose of this part of the work was to select, within a panel of proposed structures, which are the best candidates for synthesis on the basis of the predicted optical properties. Essential condition for use of these molecules (in addition to biological activity) is in fact their ability to give absorption of light in some certain range of wavelengths in the visible range. However, our main goal was not an accurate calculation of the absorption spectra (which would also require the inclusion of the vibrational contributions[21] that would be far beyond the scope of this work) but to verify the effect on the absorption band of structural modification of molecules whose optical properties were already known. Given the size of systems that prevent the use of multiconfigurational methods we chose the Time Dependent Density Functional Theory (DFT-TD) which still provides a reasonable accuracy at reasonable computational costs (time and computing resources).[22-24] There exist a wide variety of DFT functionals used in conjunction with the Time-Dependent approach[25, 26] and the chromophores in the panel of molecules proposals present different nature. Consequently, it remains difficult to know without testing what is (are) "reasonably" the most adequate functional(s) to evaluate the electronic spectra. Therefore, before to proceed with the screening, we tested six different functionals: the Long-Range Corrected hybrid GGA CAM-B3LYP,[27-30] the hybrid GGA PBE0[31-33] and mPWBW91,[34, 35] and the hybrid metaGGA Minnesota serie M06-2X, M06-HF, and M06[36-38] which differ on the weight of the Hartree-Fock exchange term. With these functional we calculated the vertical excitation energies for five chromophores structurally similar to the ones in the panel of molecules: the strigolactone **EGO-9c**[12] that was object of our previous study, the boranyl derivatives PhBorST and 4-NO_2Bor ST (Chart 2)[39]; the BODIPY dyes BODIPY HR[40] and BODIPY Et (Chart 3).[41] Results are collected in Table T **1** in SI and we chose: PBE0 (indicated by the chromophores EGO-9 and Boranyl 5 and 10) and M06 (Boranyl 5 and 10 and BODIPY 4a and 6c). These functionals present an average error of 0.09 eV and 0.08 eV, respectively. To this aim, two different series of SLs analogues were envisioned: the first series (Chart 1) was designed on the basis of our previous approach of extending the conjugation between the ABC moiety of the structure with an aromatic substituent on the A ring. In the second series, we simply functionalized our SL analogues, and some new mimics (Charts 2 and 3), with a fluorescent moiety such as a boranyl and a BODIPY (4,4-difluoro-4-bora-3a,4a-diaza-s-indacene) group, without trying to modify the electronic properties of the bioactive part of the molecule.

The spectral properties for the first series of SLs (Chart 1) were computed using PBE0 functional (see "Computational method" section for details). As reported in Table 1, only derivative EGO-9a shows intense absorption above 400 nm. Unsubstituted SL EGO-10 was added for comparison.

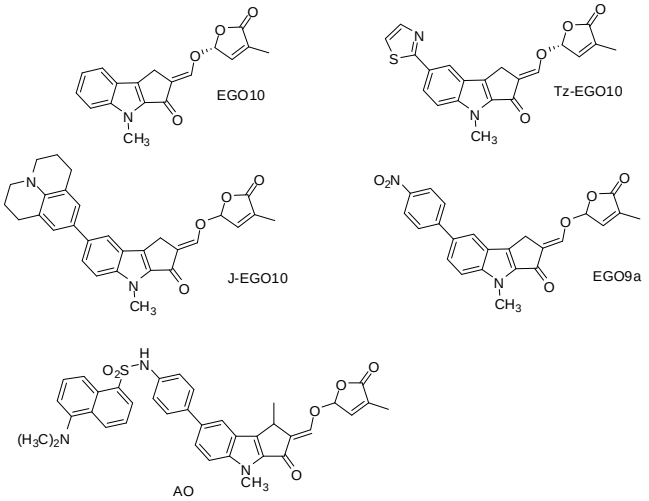

Chart 1. Strigolactones analogues

In details, we can observe (see also Figures A1-A2, SI) that all more intense (f = 0.4 ¸ 1.2, in bold in Table 1) absorptions are dominated by electronic excitation from the p molecular orbitals exclusively or mostly localized on the ABC rings to the LUMO which is a p* localized again on the ABC rings (with a large contribution of the p^*_{CO}). An important exception is EGO-9a where the p* orbital is localized on the NO_2 and whose low energy (-2.9 eV compared to 2.0 ¸ 2.1 eV) is the main responsible for the absorption above 400 nm. We can also note that in Tz-EGO10 there is a contribution of the orbitals on the thiazol substituent, but this do not improve very much the spectral properties. In J-EGO10 and AO the substituents only slightly changes the energetic of the most intense transitions.

Table 1. Calculated electronic transitions for substituted strigolactone.[a]

EGO10	TzEGO10	J-EGO10	EGO-9a	AO
355 (0.187)	380 (0.049)	464 (0.073)	**455** (0.445)	384 (0.086)
331 (0.000)	**353** (1.262)	378 (0.001)	**403** (0.503)	381 (0.243)
314 (0.747)	**326** (0.691)	**372** (0.773)	373 (0.266)	**354** (1.179)
306 (0.001)	317 (0.001)	**326** (0.840)	338 (0.778)	339 (0.001)
277 (0.001)	307 (0.001)	320 (0.536)	318 (0.003)	329 (0.004)
273 (0.145)	293 (0.436)	316 (0.001)	317 (0.003)	316 (0.001)
257 (0.001)	290 (0.012)	308 (0.001)	316 (0.045)	313 (0.001)

[a] Transitions in nm. In bold transitions commented in the text. Oscillator strengths in parenthesis. For labels see Chart 1.

Only molecule EGO-9a shows intense absorption at 455 and 403 nm and can be than considered a promising candidate for synthesis.

At this point it was clear that any simple substitution on the strigolactone analogue as a way to extend the conjugation was possibly ineffective on the spectroscopic properties we were looking for. Moreover, the experimental measures previously reported on this class of molecules showed a quantum yield too low to be detected at micromolar concentration at which the biological activity is induced. Therefore, we decided to try a different type of approach linking well known fluorescent chromophores to the strigolactone scaffold.

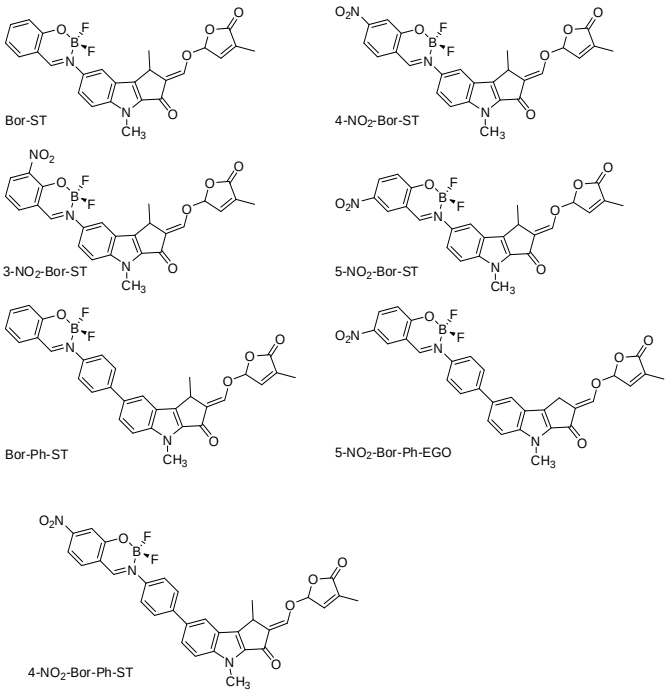

Chart 2. Boranyl-strigolactones.

The first chromophore tested was the Bor-ST (Boranyl[42] (*N*-phenyl-2,2-difluoro-1,2,3,4-tetrahydro-3-aza-2-bora-1-oxa-naphthalene) linked at position 7 of the strigolactone (Chart 2). Boranyls are a family of fluorophores based on B(III) complexes recently proposed as alternative to the original BODIPY.[43] The electronic transitions (Table 2) were calculated as the mean value obtained with the PBE0 and the M06 functionals.

Journal Name RSCPublishing

ARTICLE

Table 2. Calculated electronic transitions for Boranyl-strigolactones.[a]

Bor-ST		3-NO_2Bor-ST		5-NO_2Bor-ST		5-NO_2BorPh-EGO
	Bor-Ph-ST		4-NO2Bor-ST		4-NO_2BorPh-ST	
395 (0.402)	**402** (0.784)	**439** (0.200)	**519** (0.287)	**417** (0.254)	**537** (0.380)	**431 (0.338)**
374 (0.734)	383 (0.288)	392 (0.505)	**451** (0.425)	409 (0.095)	465 (0.211)	422 (0.319)
362 (0.336)	361 (0.631)	389 (0.051)	406 (0.108)	375 (1.106)	415 (0.077)	383 (0.251)
338 (0.555)	350 (0.301)	371 (0.468)	372 (0.362)	370 (0.071)	381 (0.160)	382 (0.134)
327 (0.142)	339 (0.125)	355 (0.223)	349 (0.052)	363 (0.061)	357 (0.543)	374 (0.231)
318 (0.003)	316 (0.001)	348 (0.314)	336 (0.742)	332 (0.453)	353 (0.855)	350 (0.697)
300 (0.001)	309 (0.001)	329 (0.509)	330 (0.114)	329 (0.560)	346 (0.008)	**337 (0.498)**

[a] Transitions in nm. In bold transitions commented in the text. Oscillator strengths *f* in parenthesis. For label see Chart 2.

The lower transitions present medium intensities (*f* = 0.2 ¸ 0.7, bold figures in Table 2), are quite intense and correspond in all cases to HOMO-LUMO transitions (see Figure B1-2, SI). Interestingly, they correspond to electron-transfer from the p molecular orbital localized on the ABC rings to a p* orbital localized on the boranyl moiety. Despite this nature, in the simplest case (Bor-ST) the transition is again below 400 nm and the addition of an aromatic ring as a spacer (Bor-Ph-ST) does not sensibly increase the wavelength. Based on what we observed for EGO-9a, we added a nitro group on the boranyl moiety. The effect on the energies of the transition (and of the molecular orbitals) is relevant (all molecules absorb above 400 nm) but strongly dependent on the position. The 4-nitro substituted (4-NO_2Bor-ST) even presents two visible transitions: 451 and 519 nm). The nitro group also affects the spectral properties of the phenyl-spaced molecules: 4-NO_2BorPh-ST presents a transition at 537 nm with good intensity while 5-NO_2BorPh-EGO at 431 nm.

Finally we tested the 1,3,5,7-tetramethyl substituted BODIPY (4,4-difluoro-4-bora-3a,4a-diaza-*s*-indacene) as fluorophore, a versatile high efficient fluorescent scaffold.[39, 41, 44] BODIPY dyes show sharp fluorescence with high quantum yield and excellent thermal and photochemical stability. Most BODIPY dyes emit from yellow to deep-red with relatively short fluorescence emission maxima (around 500 nm).[45] A large number of functional groups can be introduced to the BODIPY core and, *viceversa*, a BODIPY core can be designed and constructed on a specifically functionalized target molecule. The combination of the two approaches and well documented synthetic procedures allow a nearly unlimited structural variation.[44] The DFT functional used for the calculation was the M06 (Table 3). This time the most intense transitions were all sensibly above 400 nm. BODIPY-HR and BODIPY-EGO, obtained linking the chromophore to the SL, absorb at 486 nm. BODIPY-EG where the chromophore is directly linked to a bio-active six-membered ring, absorbs at 510 nm. Unlike the previous cases, with this chromophore the electronic excitation only involves HOMO and LUMO localized on the BODIPY moiety (see Figure C1-C2, SI). In BODIPY-HR the presence of the SL on the lower transitions is negligible (almost identical to BODIPY-Et, only added for comparison) while in BODIPY-EG the presence of the bio-active rings directly linked to the chromophore lower the energy of the LUMOs (-2.7 eV compared to -2.4 eV) increasing the absorption wavelength.

Table 3. Calculated electronic transitions for BODIPY-bioactive.[a]

BODIPY	BODIPY-Et	BODIPY-EG	BODIPY-EGO
486 (0.888)	**484** (0.884)	**510** (0.888)	**486** (0.887)
394 (0.044)	341 (0.045)	368 (0.042)	394 (0.020)
391 (0.033)	321 (0.117)	352 (0.026)	393(0.062)
366 (1.201)	281 (0.001)	350 (0.027)	365 (1.180)
345 (0.044)	271 (0.420)	337 (0.121)	345 (0.03)

[a] Transitions in nm. In bold transitions commented in the text. Oscillator strengths in parenthesis. For labels see Chart 3.

Journal Name RSCPublishing

ARTICLE

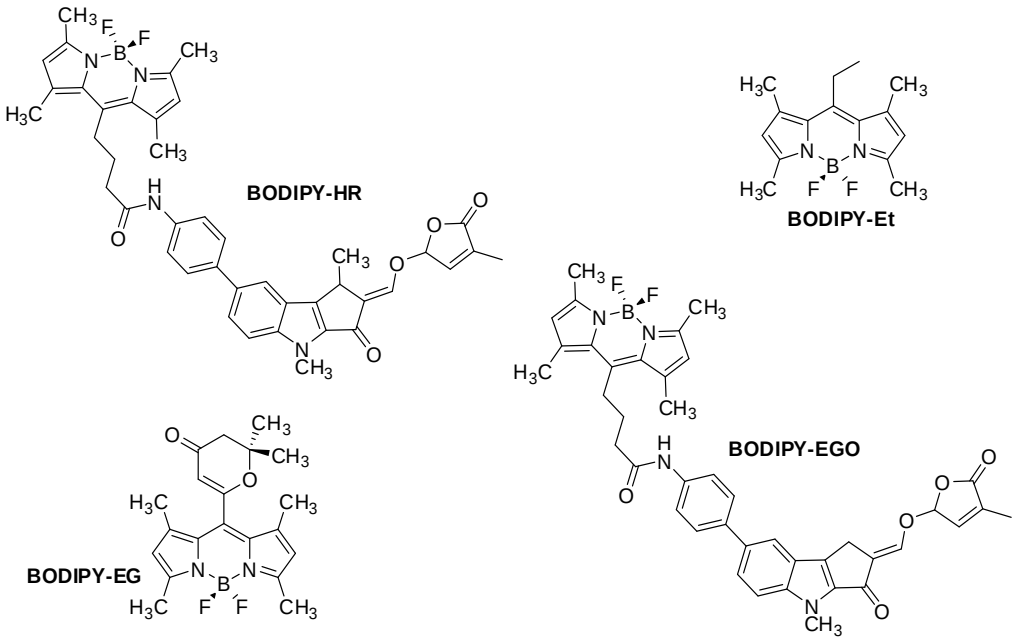

Chart 3. BODIPY-derivative bioactive

On the basis of this screening we decided to synthesize and evaluate for both spectroscopic and biological activity the following molecules: Bor-Ph-EGO, 5-NO_2BorPh-EGO (Chart 2), BODIPY-HR, BODIPY-EGO, and BODIPY-EG (Chart 3).

Compounds BODIPY-HR and BODIPY-EG have been synthesized as previously reported.[46] Bor-Ph-EGO and 5-NO_2Bor-Ph-EGO have been prepared according to the following Scheme.

Synthesis

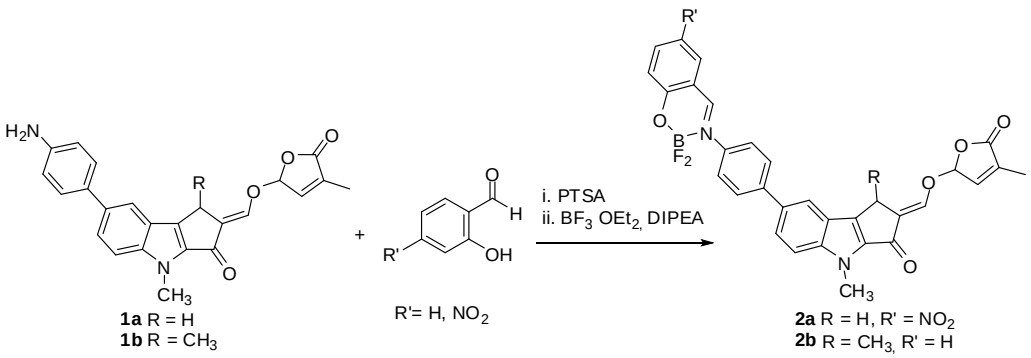

Scheme 1

Anilines **1a** and **1b**[12] were treated with salicylic aldehyde or 4-nitro salicylic aldehyde respectively in the presence of catalytic PTSA.[39] Etherated BF_3 and DIPEA were added to the newly formed imine and the mixture heated at 85 °C. Boranyls **2a** and **2b** were obtained in 32 and 55 % yield respectively.

Compound BODIPY-EGO was synthesized starting from aniline **1a** according to the following Scheme:

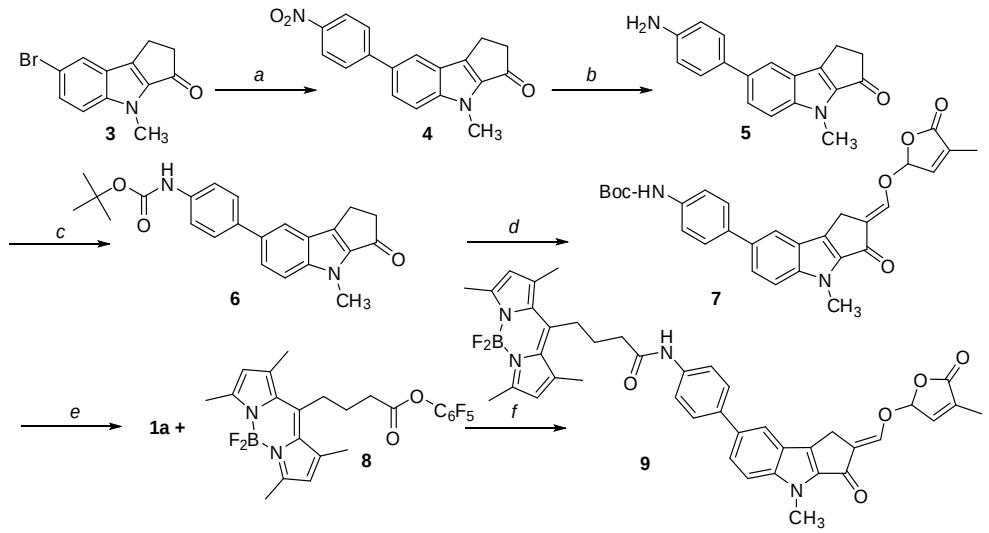

Scheme 2. Synthesis of BODIPY-EGO. (a) (p-nitropheny)boronic acid, $Pd(OAc)_2$, S-phos. K_3PO_4, THF, reflux; (b) H_2, Pd/C 10%, THF;(c) (Boc_2O), THF, reflux; (d) Ethyl formate, *t*-BuOK 1M in THF, THF, DME, bromobutenolide; (e) TFA, DCM; (f) HOBt, DMAP, CH_3CN, DMF.

Spectroscopic properties

*Spectroscopic Properties***.** Solutions of selected compounds in dichloromethane, isoabsorbent at the selected excitation wavelength were prepared and the absorption and emission spectra were acquired. In Table 4 selected photochemical properties of interest for imaging applications, as fluorescence quantum yield Φ_f and lifetimes t_f are reported. Interestingly, BODIPY derivative **HR** and **EG** show maximum excitation wavelength at 472 and 475 nm respectively (486 and 510 nm are calculated values) and high quantum yields **(Fig. 2).** Also lifetimes are consistent with bioimaging applications.

Table 4. Spectroscopic features of the synthesized compounds

Compound	λ_{exc}(nm)	λ_{em}(nm)	τ^0_f(ns), (%)[a]	τ^1_f(ns), (%)[a]	Φ_f[b]
AO	366	520			
BODIPY-HR	472	510	1.15	5.34	0.76
BODIPY-EG	475	511	5.28		0.93
BODIPY-EGO	500	518	1.27	5.16	0.76
Bor-Ph-EGO	455	565	0.48	3.15	-
5-NO_2Bor-Ph-EGO	336	518	0.66	5.97	0.63
EGO9a	360	567	0.34	3.87	

The absorption spectrum of BODIPY-EGO (See SI, A3 black line, 1.7 10^{-5}M in DCM) shows a complex and wide band: below 400 nm a max at 285, 333 and two shoulders at 305 and 370 nm are detectable. Over 400 nm the spectrum is peculiar of BODIPY group with a max at 500 nm (486 is the calculated value) and a shoulder at 470 nm. The emission spectra (A3 SI, green line, 8.5 10^{-7} M in DCM) shows the only contribution of the BODIPY at 518 nm regardless the excitation wavelength used. Being the emission signal independent from the excitation wavelength, the measurement of the quantum yield has been possible resulting in 0.76 (ref. rhodamine).

Absorption spectrum of BorPhST (see SI, A4) shows a max at 336 nm (possibly one of the three transitions calculated at 339, 350 or 360 nm) and two more peaks at 279 and 450 nm (the latter calculated at 402 nm). In this case the emission spectrum strongly depends on the excitation wavelength. At λ_{ex} 279 nm two peaks are detectable at 336 and 495. At λ_{ex} 336 nm a max at 495 nm is generated. Eventually, excitation at 450 nm induces a max in emission at 565 nm. Being the emission signal strongly dependant on the excitation wavelength the measure of quantum yield has been hampered in this case.

5-NO_2-Bor-Ph-EGO shows an absorption spectrum with a max at 336 and a shoulder at 370 nm (possibly corresponding to the calculated 337 and 350 nm). The emission spectrum is independent from the excitation wavelength and shows a max at 518 nm. Quantum yield is 0.63, lifetimes 0.66 and 5.97 respectively (corresponding to 80 and 20% of the population respectively).

In EGO 9a the max in the absorption spectra is at 336 nm with a shoulder at 360 nm (calculated, respectively, at 338 and 373 nm). The emission spectra shows a broad band from 400 to NIR and

centred at 567 nm. This feature together with the wide Stoke Shift makes this sample a very interesting candidate for biological imaging. LED excitation at 297 nm allowed the measurement of the life times. The sample shows a biexponential decay with τ_1 and τ_2 of 0.34 and 3.87 nm respectively.

Biological activity

All the new fluorescent SLs analogues have been tested for their germination activity on seeds of *Pelibancheaegyptiaca*. The activity of AO, HR and EG has already been reported and are herein represented to facilitate the comparison with the new molecules. BODIPYEGO shows a good activity at 10^{-6} and 10^{-8} molar concentration. The best concentration for BorPh-ST is 10^{-8} M. Unexpectedly, a good activity was found for BODIPY-EGO, that at 10^{-6} M is more active than GR24 (Figure 1). Good activity was found for BorPh-ST, while the nitro derivatives both 5-NO_2Bor-PhEGO and EGO-9a show a weak activity at 10^{-6} M and not activity at lower concentration.

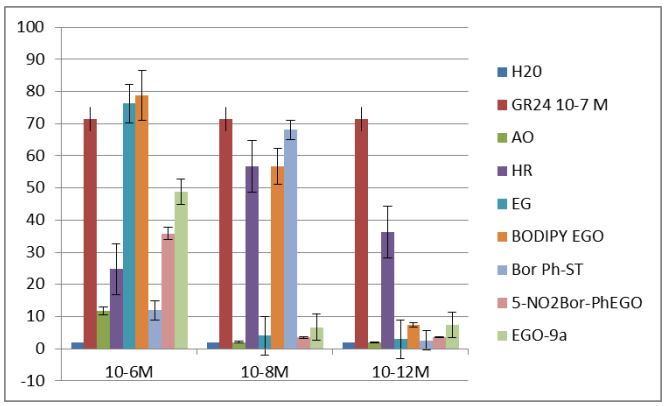

Figure 2. Percentage of germination activity of SLs fluorescent analogues on *Pelipanche aegyptiaca* seeds at different concentrations

Conclusions

This work is part of a more general study focused on the identification of the receptor of bioactive molecules known as Strigolactones. Our contribution to this topic is the design and synthesis of fluorescent labelled SLs analogues to be used as probes for the detection *in vivo* of the receptor(s). Knowledge of the putative receptor structure will boost the research on analogues of the natural substrates as required for agricultural applications. We applied a multifaceted approach aimed at selecting the best candidates as biomaging probes for *in vivo* observation. The computational screening allowed to select a reduced set of molecules to be synthesized. The spectroscopic properties have been then measured and compared with the predicted values. The agreement with the calculated spectra are sometimes not satisfactory, in particular the nitro derivatives showed a remarkable difference and the excitation maximum is generally shifted to lower wavelengths. The same molecules proved to be less active when tested for their biological activity on seeds of *Pelibancheaegyptiaca*. From the above results and considering pros and cons of each sample we pinpointed a promising candidate for our imaging studies. BODIPY-EGO can be easily synthesized, its spectroscopic properties fit with the purpose and last but not least its biological activity is perfectly in line with the universal standard GR24. Preliminary observations on biological samples are presently ongoing and confirm expectations.

Experimental

Calculations

Density Functional Theory (DFT)[47, 48] was also exploited for geometry optimization with the 6-31+G(d)[49, 50] basis set. Solvent effects were introduced both in geometry optimisation and Time-Dependent DFT calculations by the Polarized Continuum Method (PCM)[51-54] within the universal Solvation Model Density.[55, 56] Calculations were performed by the quantum package Gaussian 09-A.[57] Figures in SI were obtained with the graphical program Molden.[58]

Synthesis

General procedure for 2a and 2b. To a solution of aniline **1a, 1b**(1 eq.) and PTSA (one crystal) in dry ethanol was added the appropriate aldehyde (1 eq.). The resulting solution was refluxed overnight. After cooling down, the desired *anyl* precipitates. The precipitate was then filtered, washed with ethanol, pentane and dried under vacuum. To a stirred solution of *anyl* (1eq.) in dry dichloroethane at 85°C was added $BF_3{\cdot}OEt_2$ (2.5 eq.). A colour change occurs or a precipitate appears revealing the formation of an intermediate. Then DIEA (2.5 eq.) is added to form the desired *boranyl*. The course of reaction was monitored by TLC analysis. After cooling down, the reaction mixture was washed with a saturated solution of $NaHCO_3$ and extracted with dichloromethane. Organic layers were dried over $MgSO_4$ and evaporated under vacuum . The product was purified by silica gel chromatography. **2a**. Yellow powder. Yield: 32%. ^{1}H NMR (200 MHz, $CDCl_3$) δ (ppm): 8.42 (1H, s, C*H* Imine), 8.32 (1H, CH arom), 7.65 (2H, d *J* = 7.3 Hz C*H*Arom), 7.55 (m, 3H arom), 7.39 (2H, d *J*= 7.3 Hz, C*H*arom), 7.28 (1H, C*H* arom), 7.05 (m, 2H, C*H*arom), 6.97 (1H, d *J*= 5 Hz, C*H*O), 6.95 (1H, s), 3.96 (3H, s, *N*Me), 3.56 (2H, s), 2.43 (3H s); ^{13}C NMR (75 MHz, $CDCl_3$) δ (ppm): 179.2 (s), 170.8 (s), 167.6 (s), 163,7 (d, C=N), 163.7 (d), 152.4 (s), 144.4 (s), 143.1 (s), 141.3 (s), 141.2 (s), 139.8 (s), 133.4 (s), 132.4 (d), 131.8 (d), 129.9 (2C, d), 128.9 (d), 125,7 (d), 122.8 (d), 123.2 (d), 121.3 (s), 119.5 (s), 116.9 (2C, d), 112.1 (d), 105.3 (s), 94.5 (d), 34.5 (q), 23.9 (t), 20.8 (q).; Anal. Calcd for $C_{31}H_{22}BF_2N_3O_7$: C, 62.33; H, 3.71; N, 7.03; Found : C, 62.62; H, 3.42; N, 7.09; EI-MS (*m/z*) : 597.0 (18), 484 (28), 308 (18), 113 (56). **2b** whitish powder. Yield 55%. ^{1}H NMR (200 MHz, $CDCl_3$) δ (ppm): 8.38 (1H, s, CH Imine), 7.65 (1H, d *J* = 7.3 Hz C*H*Arom), 7.66 (1H, d *J*= 7.3 Hz, C*H*arom), 7.55 (m, 5H arom), 7.39 (2H, d *J*= 7.3 Hz, C*H*arom), 7.34 (1H, d *J*= 7.3, C*H*arom), 7.05 (m, 4H, C*H*arom), 6.95 (1H, d *J*= 5 Hz, CH arom), 3.96 (3H, s, *N*Me), 3.63 (1H, q *J*= 5.8 Hz), 2.43 (3H s), 1.53 (3H d *J*= 5.8 Hz); ^{13}C NMR (75 MHz, $CDCl_3$) δ (ppm): 177.2 (s), 170.1 (s), 163,4 (d, C=N), 162.7 (d), 160,2 (s), 152.4 (s), 144.7 (d), 143.7 (s), 142.3 (s),

140.8 (s), 139.3 (s), 132.4 (s), 132.4 (d), 130.3 (s), 129.2 (2C, d), 128.4 (s), 125,1 (s), 123.2 (2C, d), 122.8 (d), 121.4 (d), 119.4 (d), 118.5 (s), 118.2 (d), 116.1 (d), 111.0 (d), 109. 2 (s), 93.9 (d), 32.3 (q), 27.9 (d), 20.8 (q), 18.8 (q).; Anal. Calcd for $C_{32}H_{26}BF_2N_2O_5$: C, 61.63; H, 4.13; N, 6.86; Found : C, 61.58; H, 4.12; N,6.82; EI-MS (*m/z*) : 566.0 (12), 453 (15), 264 (55), 113 (80).

4-methyl-7-(4-nitrophenyl)-1,2-dihydrocyclopenta[b]indol-3(4H)-one (4): to a suspension of K_3PO_4 (2.44 g, 11.48 mmol) and (*p*-nitrophenyl)boronic acid (1.44 g, 8.61 mmol) in anhydrous THF (60 mL), substrate **3** (759 mg, 2.87 mmol), $Pd(OAc)_2$ (32 mg, 0.144 mmol) and S-Phos (118 mg, 0.287 mmol) was added under nitrogen atmosphere. The red reaction mixture was refluxed and monitored by TLC (AcOEt/hexane 2:5, R_f = 0.24). After complete consumption of the substrate (3.5 h) the mixture was cooled to room temperature, diluted with H_2O (170 mL) and extracted with AcOEt (3x80 mL). The combined organic phases were dried over Na_2SO_4. After filtration and evaporation of the solvent, column chromatography (DCM/MeOH 60:1, R_f = 0.48) gave product **4** (871 mg, 2.84 mmol, 99%) as yellow solid. ^{1}H NMR (200 MHz, CDCl3) δ: 8.32 (d, 2H), 7.97 (d, 1H), 7.80 (d, 2H), 7.70 (dd, 1H), 7.48 (d, 1H), 3.97 (s, 3H), 3.14-3.11 (m, 2 H), 3.05-3.01 (m, 2H).

7-(4-aminophenyl)-4-methyl-1,2-dihydrocyclopenta[b]indol-3(4H)-one (5): to a solution of nitro compound **4** (50.7 mg, 0.165 mmol) in anhydrous THF (5.5 mL), was added Pd/C 10% (10.5 mg) under nitrogen atmosphere. The reaction was let stirred under hydrogen atmosphere for 2.5 h. The mixture was filtered through Celite and the filter was washed with THF. The solvent was evaporated and the crude product (53 mg) was use in the next step.^{1}H NMR (400 MHz, $CDCl_3$) δ: 7.81 (d, 1H), 7.62 (dd, 1H), 7.45 (d, 2H), 7.38 (d, 1H), 6.78 (d, 2H), 3.93 (s, 3H), 3.72 (bs, 1H), 3.09-3.07 (m, 2H), 3.01-2.98 (m, 2H) ppm.

***Tert*-butyl 4-(4-methyl-3-oxo-1,2,3,4-tetrahydrocyclopenta[b]indol-7-yl)phenylcarbamate (6)**: a mixture of crude free amine **5** (53 mg) and di-*tert*-butyl dicarbonate (109 mg) was heated under reflux in THF (10 ml) overnight. The mixture was cooled to rt and THF was removed under reduced pressure. The residue was dissolved in AcOEt (40 mL), washed with water (30 mL), dried under Na_2SO_4, and concentrated to dryness. After purification by column chromatography (AcOEt/esano 1:2, R_f: 0.34) 47 mg of **6** (0.126 mmol, 76% over two steps) was obtained as yellow solid. m.p. 217.7-219.5 °C. ^{1}H NMR (400 MHz, $CDCl_3$) δ: 7.85 (d, J = 1.2 Hz, 1H), 7.64 (dd, J = 8.8, 1.8 Hz, 1H), 7.57 (d, J = 8.6 Hz, 2H), 7.45 (d, J = 8.6 Hz, 2H), 7.41 (d, J = 8.8 Hz, 1H), 3.94 (s, 3H), 3.11-3.09 (m, 2H), 3.02-3.00 (m, 2H), 1.55 (s, 9H) ppm. ^{13}C NMR (50 MHz, $CDCl_3$) δ: 194.9 (C=O), 152.8 (C=O), 145.2 (Cq_{arom}), 144.3 (Cq_{arom}), 138.3 (Cq_{arom}), 137.3 (Cq_{arom}), 136.4 (Cq_{arom}), 133.3 (Cq_{arom}), 127.8 (2 x CH_{arom}), 126.5 (CH_{arom}), 123.6 (Cq_{arom}), 119.6 (CH_{arom}), 119.0 (2 x CH_{arom}), 111.3 (CH_{arom}), 80.8 ($C(CH_3)_3$), 41.7 (CH_2CO), 30.4 (NCH_3), 28.5 ($C(CH_3)_3$), 19.8 (CH_2CH_2CO) ppm. MS (ESI): *m/z* (%) = 377.2 (100) $[M + H]^+$.

(E)-tert-butyl 4-(4-methyl-2-((4-methyl-5-oxo-2,5-dihydrofuran-2-yloxy)methylene)-3-oxo-1,2,3,4-tetrahydrocyclopenta[b]indol-7-yl)phenylcarbamate (7): to a suspension of compound **6** (105 mg, 0.28 mmol) in anhydrous THF (3 mL), cooled to 0°C and under nitrogen atmosphere, were added ethyl formate (7 mL) and, dropwise, a 1 M solution of *t*BuOK (2 mL, 2 mmol) in THF. The reaction mixture was left stirring at room temperature with monitoring by TLC (*n*-hexane/EtOAc, 3:2). After complete consumption of the substrate (3 h), the solvent was evaporated under strong nitrogen flow rendering a solid residue to which were added anhydrous DME (5 mL) and, after cooling to 0°C, bromobutenolide (310 mg, 1.7 mmol). The resulting mixture was left while stirring at room temperature for 16 h and than diluited with AcOEt (15 mL) and quenched by addition of a saturated NH_4Cl aqueous solution (15 mL). The mixture was extracted with AcOEt (2 x15 mL) and the combined organic layer was dried over Na_2SO_4. After filtration and evaporation of the solvent, chromatography (CH_2Cl_2/MeOH 70:1, R_f = 0.3) gave compound **7** (100 mg, 0.2 mmol, 71%) in 71% yeld. ^{1}H NMR (400 MHz, $CDCl_3$) δ: 7.81 (d, J = 1.4 Hz, 1H), 7.62 (dd, J = 8.8, 1.8 Hz, 1H), 7.57 (s, 1H), 7.55 (s, 2H), 7.46 (s, 2H), 7.42 (d, J = 7.2 Hz, 1H), 6.98 (t, J = 1.6 Hz, 1H), 6.53 (bs, 1H), 6.21 (t, J = 1.4 Hz, 1H), 3.98 (s, 3H), 3.63 (s, 2H), 2.04 (t, J = 1.5 Hz, 3H), 1.54 (s, 9H) ppm. ^{13}C NMR (50 MHz, $CDCl_3$) δ: 182.9 (C=O), 170.7 (C=O), 152.9 (COO), 146.3 (C=*C*HO), 143.9 (Cq_{arom}), 143.3 (Cq_{arom}), 141.5 (CH_3C=*C*H), 140.3 (Cq_{arom}), 137.5 (Cq_{arom}), 136.4 (Cq_{arom}), 135.7 (Cq_{arom}), 133.6 (CH=*C*CH_3), 129.7 (Cq_{arom}), 127.8 (CH_{arom} d, 2C), 126.4 (CH_{arom}, 2C), 122.8 (*C*=CHO), 119.5 (CH_{arom}), 119.1 (CH_{arom}), 111.3 (CH_{arom}), 100.9 (OCHO), 80.7 (($CH_3)_3C$), 30.4 (NCH_3), 28.5 (3C, (($CH_3)_3$C)), 21.6 (CH_2), 10.8 (CH_3C=) ppm.

(E)-7-(4-aminophenyl)-4-methyl-2-((4-methyl-5-oxo-2,5-dihydrofuran-2-yloxy)methylene)-1,2-dihydrocyclopenta[b]indol-3(4H)-one (1a): compound **7** (96.9 mg, 0.19 mmol) was dissolved in anhydrous DCM and treated with TFA (222 μL) at 0°C. The reaction was stirred for 30 min at 0°C and than at r.t. for another 30 min. Afterwards, $NaHCO_3$ sat. (15 mL) was carefully added and the aqueous phase was extracted with DCM (4x15 mL). The organic layer was dried over Na_2SO_4 and the solvent was evaporated under reduced pressure to give **1a** (73 mg, 0.18 mmol, 96%). ^{1}H NMR (400 MHz, $CDCl_3$) δ: 7.81 (d, 1H), 7.62 (dd, 1H), 7.57-7.55 (m, 3H), 7.46-7.42 (m, 3H), 6.98 (t, 1H), 6.53 (bs, 1H), 6.21 (t, 1H), 3.98 (s, 3H), 3.63 (s, 2H), 2.04 (t, 3H), 1.54 (s, 9H) ppm.

BODIPY-EGO: in a two neck flask, the free amine **1a** (73 mg, 0.18 mmol) was suspended in dry acetonitrile (20 mL). Then, ester **8**[46] (108 mg, 0.22 mmol) and HOBt (27.6 mg, 0.18 mmol) were added and the mixture was stirred overnight. DMF (8 mL) and DMAP (30 mg, 0.25 mmol) were added and the reaction was stirred for 36 h. Acetonitrile was removed and H_2O (80 mL) was added. The product was extract in CH_2Cl_2 (40 mL) and the organic layer was washed with H_2O (1x80 mL, 1x40 mL) and dried over Na_2SO_4. After filtration and evaporation of the solvent, purification by column chromatography on silica (AcOEt/hexane 2:1, R_f: 0.32) gave the compound as a bright red solid (10.8 mg, 0.015 mmol, 8%). ^{1}H NMR (400 MHz, CDCl3) δ: 7.82 (s, 1H), 7.7-7.4 (m, 5H), 7.21-7.17 (m, 2H), 6.98 (s, 1H), 6.21 (s, 1H), 6.06 (s, 2H), 3.99 (s, 3H), 3.63

(s, 2H), 3.14-3.10 (m, 2H), 2.86 (t, 2H), 2.52 (s, 6H), 2.46 (s, 6H), 2.17-2.06 (m, 2H), 2.04 (s, 3H) ppm. ^{13}C NMR (100.4 MHz, $CDCl_3$) δ: 183.1 (*C*=O), 170.5 (*C*OO), 169.8 (*C*ONH), 154.2 (Cq_{arom}), 146.1 (*C*H=CCH$_3$), 145.5 (Cq_{arom}), 143.7 (Cq_{arom}), 143.0 (Cq_{arom}), 141.3 (C=*C*H), 140.4 (Cq_{arom}), 140.0 (Cq_{arom}), 136.5 (Cq_{arom}), 135.6 (Cq_{arom}), 135.4 (Cq_{arom}), 133.9 (Cq_{arom}), 133.2 (Cq_{arom}), 131.6 (CH=*C*CH$_3$), 128.8 (Cq_{arom}), 128.2 (Cq_{arom}), 127.7 (CH_{arom}), 126.2 (CH_{arom}), 123.9 (CH_{arom}), 123.2 (CH_{arom}), 121.9 (*C*=CH), 120.2 (2xCH_{arom}), 119.5 (CH_{arom}), 115.3 (Cq_{arom}), 111,4 (CH_{arom}), 100.6 (O-*C*H-O), 37.2 (*C*H$_2$C=O), 30.4 (N*C*H$_3$), 29.7 (2xCH_2), 17.3 (2xN=C*C*H$_3$), 16.5 (C=C*C*H$_3$), 14.5 (C=C*C*H$_3$), 10.7 (CH=C*C*H$_3$) ppm.

Biological Activity: Plant material. Seeds of *Orobanche aegyptiaca* were collected from field grown tomato in the West Galilee of Israel. The seeds were stored in glass vials in the dark at room temperature until use in germination tests. Preparation of test solutions: the compound to be tested was weighted and dissolved in 1 mL of acetone and then diluted with sterile distilled water to reach the desired concentrations. All solutions were prepared just before use. Seeds were surface sterilized and preconditioned according to Bhattacharya et al., 2009. Briefly seeds were exposed for 5 min to 50% (v/v) aqueous solutions of commercial bleach (2% hypochlorite) and rinsed with sterile distilled water. For preconditioning seeds were sown by using a sterile toothpick on a glass fibre filter paper disc (approximately 20 seeds per disc), the glass fibre discs were placed on 2 filter paper discs, wetted with sterile distilled water and incubated at 25 °C in the dark for 6 days. The preconditioned seeds were then allowed to dry completely (under the hood) in the laminar flow, treated with the strigolactones analogues solutions at 5 different concentrations: 10^{-4} M, 10^{-6} M, 10^{-8} M, 10^{-10} M and 10^{-12} M and the germination rate was evaluated under a stereomicroscope 7 days after treatment. For each concentrations at least 100 seeds were analyzed, synthetic strigolactone GR24 (10^{-7} M) was purchased from Strigolab s.r.l. and included as positive control, while an aqueous solution of 0.1% acetone and sterile distilled water were included as negative control. Seeds were considered to be germinated if the radicle protruded through the seed coat.

Acknowledgements
This study stem from the STREAM project, "Strigolactones enhances Agricultural Methodologies" which is funded as a EU COST Action-COST fa1206." We are particularly grateful to Dr. Hinanit Koltai and Dr. Manoj Kumar of the ARO Volcani Center (IL) for confocal microscopy observations and helpful discussion.

Notes and references

[a] Dipartimento di Chimica, Università di Torino, via P. Giuria 7-10125 Torino, Italy
[b] Dipartimento di Chimica "Ugo Schiff", Università di Firenze, via della Lastruccia 13, 50019 Sesto Fiorentino (FI), Italy
[c]Dipartimento di Scienze della Vita e Biologia dei Sistemi, Viale Mattioli 25, 10125 Torino, Italy

Electronic Supplementary Information (ESI) available: [details of any supplementary information available should be included here]. See DOI: 10.1039/b000000x/

1. J. A. Lopez-Raez, T. Charnikhova, V. Gomez-Roldan, R. Matusova, W. Kohlen, R. De Vos, F. Verstappen, V. Puech-Pages, G. Becard, P. Mulder and H. Bouwmeester, *New Phytol.*, 2008, **178**, 863-874.
2. M. Umehara, A. Hanada, S. Yoshida, K. Akiyama, T. Arite, N. Takeda-Kamiya, H. Magome, Y. Kamiya, K. Shirasu, K. Yoneyama, J. Kyozuka and S. Yamaguchi, *Nature*, 2008, **455**, 195-U129.
3. H. Koltai, *New Phytol*., 2011, **190**, 545-549.
4. W. Kohlen, T. Charnikhova, Q. Liu, R. Bours, M. A. Domagalska, S. Beguerie, F. Verstappen, O. Leyser, H. Bouwmeester and C. Ruyter-Spira, *Plant Physiol.*, 2011, **155**, 974-987.
5. A. S. Mwakaboko and B. Zwanenburg, *Biorg. Med. Chem.*, 2011, **19**, 5006-5011.
6. K. Akiyama, K. Matsuzaki and H. Hayashi, *Nature*, 2005, **435**, 824-827.
7. E. Foo and N. W. Davies, *Planta*, 2011, **234**, 1073-1081.
8. C. B. Pollock, H. Koltai, Y. Kapulnik, C. Prandi and R. I. Yarden, *Breast Cancer Research and Treatment*, **134**, 1041-1055.
9. D. C. Nelson, A. Scaffidi, E. A. Dun, M. T. Waters, G. R. Flematti, K. W. Dixon, C. A. Beveridge, E. L. Ghisalberti and S. M. Smith, *Proceedings of the National Academy of Sciences of the United States of America*, 2011, **108**, 8897-8902.
10. K. Akiyama, S. Ogasawara, S. Ito and H. Hayashi, Plant and *Cell Physiology*, 2010, **51**, 1104-1117.
11. X. N. Xie and K. Yoneyama, *Annual Review of Phytopathology*, Vol 48, 2010, **48**, 93-117.
12. C. Prandi, E. G. Occhiato, S. Tabasso, P. Bonfante, M. Novero, D. Scarpi, M. E. Bova and I. Miletto, *Eur. J. Org. Chem.*, 2011, 3781-3793.
13. H. Malik, F. Rutjes and B. Zwanenburg, *Tetrahedron*, 2010, **66**, 7198-7203.
14. A. Reizelman, M. Scheren, G. H. L. Nefkens and B. Zwanenburg, *Synthesis-Stuttgart*, 2000, 1944-1951.
15. J. Thuring, N. Heinsman, R. Jacobs, G. H. L. Nefkens and B. Zwanenburg, *J. Agric. Food. Chem.*, 1997, **45**, 507-513.
16. A. S. Mwakaboko and B. Zwanenburg, *Plant and Cell Physiology*, 2011, **52**, 699-715.
17. H. Koltai, M. Cohen, O. Chesin, E. Mayzlish-Gati, G. Becard, V. Puech, B. Ben Dor, N. Resnick, S. Wininger and Y. Kapulnik, *J. Plant Physiol.*, 2011, **168**, 1993-1996.
18. F.-D. Boyer, A. d. S. Germain, J.-P. Pillot, J.-B. Pouvreau, V. X. Chen, S. Ramos, A. Stevenin, P. Simier, P. Delavault, J.-M. Beau and C. Rameau, *Plant Physiol*., 2012, **159**, 1524-1544.
19. T. Asami and S. Ito, *J.Synt. Org. Chem.* Japan, 2012, **70**, 36-49.

20. C. Bhattacharya, P. Bonfante, A. Deagostino, Y. Kapulnik, P. Larini, E. Occhiato, C. Prandi and P. Venturello, *Org. Biomol. Chem*, 2009, **7**, 3413-3420.
21. D. Jacquemin, A. Planchat, C. Adamo and a. B. Mennucci, J. *Chem. Theory Comput.*, 2012, **8**, 2359−2372.
22. A. Dreuw and a. M. Head-Gordon, *Chem. Rev.*, 2005, **105**, 4009-4037.
23. R. Bauernschmitt and a. R. Ahlrichs, *Chem. Phys. Lett.*, 1996, **256**, 454-464.
24. E. Runge and E. K. U. Gross, *Phys. Rev. Lett.*, 1984, 52, 997–1000.
25. D. Jacquemin, E. A. Perpète, O. A. Vydrov, G. E. Scuseria and C. Adamo, *J. Chem. Phys.*, 2007, **127**, Art. 094102.
26. D. Jacquemin, V. Wathelet, E. A. Perpète and C. Adamo, *J. Chem. Theory Comput.* , 2009, **5**, 2420–2435.
27. T. Yanai, D. P. Tew and N. C. Handy, *Chem. Phys. Lett.*, 2004, **393**, 51–57.
28. T. Yanai, R. J. Harrison and N. C. Handy, *Mol. Phys*., 2005, **103**, 413–424.
29. M. J. G. Peach, A. J. Cohen and D. J. Tozer, *Phys. Chem. Chem. Phys.*, 2006, **8**, 4543–4549.
30. M. J. G. Peach, T. Helgaker, P. Salek, T. W. Keal, O. B. Lutnaes, D. J. Tozer and N. C. Handy, *Phys. Chem. Chem. Phys*, 2006, **8**, 558–556.
31. M. Ernzerhof and G. E. Scuseria, *J. Chem. Phys*., 1999, **110**, 5029–5036.
32. C. Adamo and V. Barone, *J. Chem. Phys*, 1999, **110**, 6158–6169.
33. J. P. Perdew, M. Ernzerhof and K. Burke, *J. Chem. Phys*., 1996, **105**, 9982–9985.
34. C. Adamo and V. Barone, *J. Chem. Phys*., 1998, **108**, 664–675.
35. J. P. Perdew, *Electronic Structure of Solids '91*, ed. P. Ziesche and H. Eschrig, AkademieVerlag, Berlin, 1991, 11-20.
36. Y. Zhao and D. G. Truhlar, *Acc. Chem. Res.*, 2008, **41**, 157–167.
37. Y. Zhao and D. G. Truhlar, *J. Phys. Chem. A*, 2006, **110**, 13126–13130.
38. Y. Zhao and D. G. Truhlar, *Theor. Chem. Account*, 2008, **120**, 215–241.
39. D. Frath, S. Azizi, G. Ulrich, P. Retalleau and R. Ziessel, *Org. Lett.*, 2011, **13**, 3414-3417.
40. V. Leen, D. Miscoria, S. Yin, A. Filarowski, J. M. Ngongo, M. V. d. Auweraer and W. D. N. Boens, *J. Org. Chem*., 2011, **76**, 8168-8176.
41. C. Yu, L. Jiao, H. Yin, J. Zhpu, W. Pang, Y. Wu, Z. Wang, G. Yang and E. Hao, *Eur. J. Org. Chem*., 2011, 5460-5468.
42. A. Treibs and F. H. Kreuzer, *Liebigs Ann. Chem.*, 1968, **718**, 208-223.
43. L. Yuan, W. Lin, K. Zheng, L. He and W. Huang, *Chem. Soc. Rev*., 2013, **42**, 622-661.
44. N. Boens, V. Leen and W. Dehaen, *Chem. Soc. Rev.*, 2012, **41**, 1130-1172.
45. S. Luo, E. Zhang, Y. Su, T. Cheng and C. Shi, *Biomaterials*, 2011, **32**, 7127-7138.
46. C. Prandi, H. Rosso, B. Lace, E. G. Occhiato, A. Oppedisano, S. Tabasso, G. Alberto and M. Blangetti, *Mol. Plant*, 2013, **6**, 113-127
47. R. G. Parr and W. Yang, *Density Functional Theory of Atoms and Molecules* Oxford University Press: New York1989.
48. W. Kohn, A. D. Becke and R. G. Parr, *J. Phys. Chem.*, 1996, **100**, 12974-12980.
49. W. J. Hehre, R. Ditchfield and J. A. Pople., *J. Chem. Phys.*, 1972, **56**, 2257–2261.
50. J. C. T. Clark, G. W. Spitznagel, and P. v. R. Schleyer*J. Comp. Chem.*, 1983, **4**, 294–301.
51. M. Cossi, N. Rega, G. Scalmani and V. Barone, *J. Chem. Phys*., 2001, **114**, 5691–5570.
52. V. Barone and M. Cossi, *J. Phys. Chem. A*, 1998, **102**, 1995–2001.
53. M. T. Cancès, B. Mennucci and J. Tomasi, *J. Chem. Phys*., 1997, **107**, 3032–3041.
54. B. Mennucci and J. Tomasi, *J. Chem. Phys.*, 1997, **106**, 5151–5158.
55. A. V. Marenich, C. J. Cramer and D. G. Truhlar, J. Phys. Chem. B, 2009, **113**, 6378–6396.
56. A. V. Marenich, C. J. Cramer and D. G. Truhlar, *J. Phys. Chem. B*, 2009, **113**, 4538–4543.
57. R. A. Gaussian 09, M. J. Frisch, G. W. Trucks, H. B. Schlegel, G. E. Scuseria, M. A. Robb, J. R. Cheeseman, G. Scalmani, V. Barone, B. Mennucci, G. A. Petersson, H. Nakatsuji, M. Caricato, X. Li, H. P. Hratchian, A. F. Izmaylov, J. Bloino, G. Zheng, J. L. Sonnenberg, M. Hada, M. Ehara, K. Toyota, R. Fukuda, J. Hasegawa, M. Ishida, T. Nakajima, Y. Honda, O. Kitao, H. Nakai, T. Vreven, J. A. Montgomery, Jr., J. E. Peralta, F. Ogliaro, M. Bearpark, J. J. Heyd, E. Brothers, K. N. Kudin, V. N. Staroverov, R. Kobayashi, J. Normand, K. Raghavachari, A. Rendell, J. C. Burant, S. S. Iyengar, J. Tomasi, M. Cossi, N. Rega, J. M. Millam, M. Klene, J. E. Knox, J. B. Cross, V. Bakken, C. Adamo, J. Jaramillo, R. Gomperts, R. E. Stratmann, O. Yazyev, A. J. Austin, R. Cammi, C. Pomelli, J. W. Ochterski, R. L. Martin, K. Morokuma, V. G. Zakrzewski, G. A. Voth, P. Salvador, J. J. Dannenberg, S. Dapprich, A. D. Daniels, Ö. Farkas, J. B. Foresman, J. V. Ortiz, J. Cioslowski, and D. J. Fox, Gaussian, Inc., Wallingford CT, 2009.
58. G. Schaftenaari and J. H. Noordik, *J. Comput.-Aided Mol. Design*, 2000, **14**, 123–134.

Tailoring Fluorescent Strigolactones for *in vivo* Investigations: a computational and experimental study

Cristina Prandi, Giovanni Ghigo, Ernesto G, Occhiato, Dina Scarpi, Stefano Begliomini, Beatrice Lace, Gabriele Alberto, Emma Artuso, Marco Blangetti

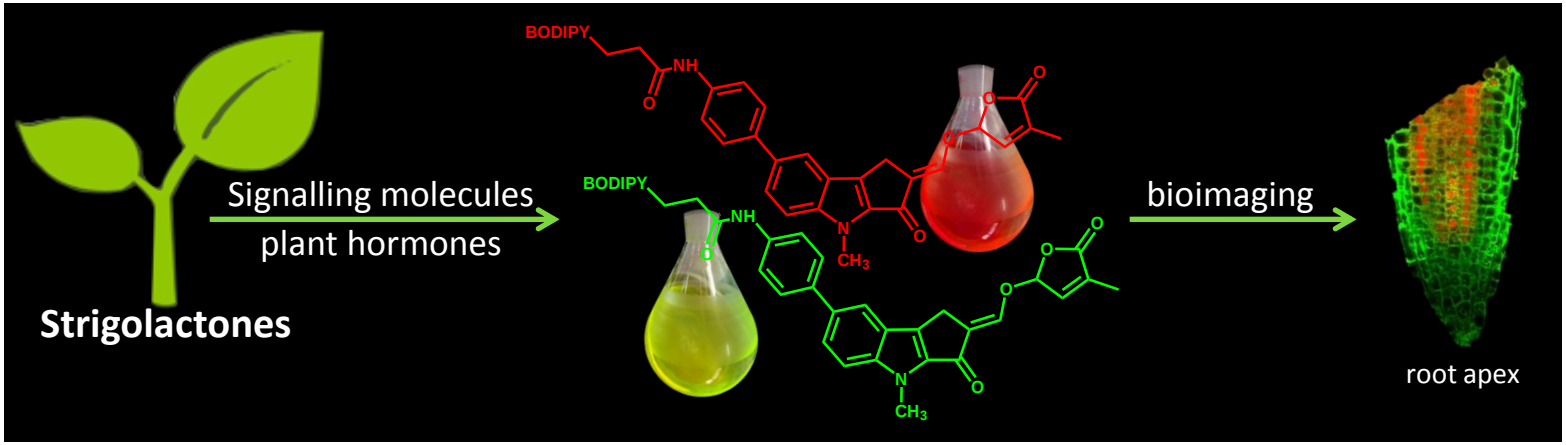

Fluorescent Strigolactones have been designed and synthesized to fit bioimaging requirements